Journal of Energy and Natural Resources
2026, Vol. 15, No. 2, pp. 51–63
https://doi.org/10.11648/j.jenr.20261502.12

Research Article

Evaluation of Lateritic Iron Deposits in the Jimma Zone, South-Western Ethiopia: Geology, Mineralogy, Geochemistry and Resource Potential

Yirgalem Hunegnaw*, Mekdes Taye, Tewodros Tilahun, Habtamu Adugna, Tadesse Tsehaw, Ashenafi Yazew, Dessalew Mengistie

Geological Institute of Ethiopia, Ministry of Mines, Addis Ababa, Ethiopia

Abstract

Lateritic iron deposits are widespread on the Ethiopian plateau but remain largely unevaluated. This study presents an integrated geological, mineralogical and geochemical assessment of seven lateritic iron occurrences in the Omo Beyem and Nedi Gibe woredas of the Jimma Zone, south-western Ethiopia. The deposits are hosted by Tertiary volcanic rocks (basalt, rhyolite, and trachyte) of the Jimma Volcanics and occur as massive duricrust caps, stockwork veins, and ferruginous coatings on felsic volcanics. Reflected-light petrography reveals an ore mineralogy dominated by hematite (30–60%) and goethite (10–35%) with minor magnetite (0.5–5%). Whole-rock major-oxide analyses of 131 samples from trenches, pits and outcrops yield Fe_2O_3 contents ranging from 7.0 wt.% to 70.7 wt.% (overall mean 48.33 wt.%). The highest grades are recorded at Demboba (mean 52.38% Fe_2O_3) and Chucha Serado (mean 63.00% Fe_2O_3). The Chemical Index of Alteration (CIA) of 88.5–89.2%, together with the near-complete leaching of alkali and alkaline-earth elements, indicates intense tropical weathering. A ternary SiO_2–Al_2O_3–Fe_2O_3 diagram classifies the ores as products of moderate to strong lateritization. Resource estimation based on detailed mapping (1:5,000 scales), pitting, and trenching and bulk-density measurements yield an indicated total resource of approximately 2.7 million tonnes of contained iron metal. The results establish the Jimma laterites as a medium-grade iron resource suitable for small-scale industrial exploitation and significantly expand the known lateritic iron province of the Ethiopian plateau southward.

Keywords

Lateritic Iron, Jimma Zone, Ethiopian Plateau, Geochemistry, Mineralogy, Supergene Enrichment, Cenozoic Volcanism, CIA Weathering Index

1. Introduction

Iron is the world's most consumed metal and a cornerstone of industrial development. Kim, Y. et al [28] In Ethiopia, domestic iron-ore production are negligible, and the country depends entirely on imported steel to meet the demands of its growing construction and manufacturing sectors. The Ethiopian plateau, however, hosts numerous lateritic iron occurrences that have been known and locally smelted for centuries [22]. Systematic investigations of deposits such as

*Correspondence: Yirgalem Hunegnaw (yirgalemgeol@gmail.com)

Received: 5 May 2026; **Accepted:** 2 July 2026; **Published:** 22 July 2026

Mekaneselam in the north-western plateau [17]. Mai-Kuhli in western Tigray [21] and Mentebteb in the north [45] have demonstrated that these laterites formed through deep chemical weathering of ferruginous volcanic protoliths during the prolonged tropical Peneplanation intervals of the Cenozoic. Other documented occurrences include ferricrete near Shire [26], the Negash deposit [1] and the Bikilal magnetite–ilmenite deposit in West Wollega [29].

The Jimma Zone geographically located at (7°40′ N, 36°50′ E) in south-western Ethiopia is underlain by the Jimma Volcanics a thick succession of Oligocene–Miocene basalts, trachytes, rhyolites and ignimbrites [31, 16]. The region experiences a warm, humid climate with annual rainfall of 1200–2400 mm and mean temperatures of 11–25°C, providing ideal conditions for lateritization [38]. Historical records indicate that iron was smelted in the Jimma area during the 19th century under the kingdom of Jimma Aba Jiffar, and that during the Italian occupation (1937–1938) small blast furnaces at Gato and Chefeneqa reportedly produced several tonnes of crude iron [25]. Despite this long history of exploitation, no comprehensive geological, mineralogical or geochemical evaluation of the iron resources of the Jimma Zone has been published prior to the present work.

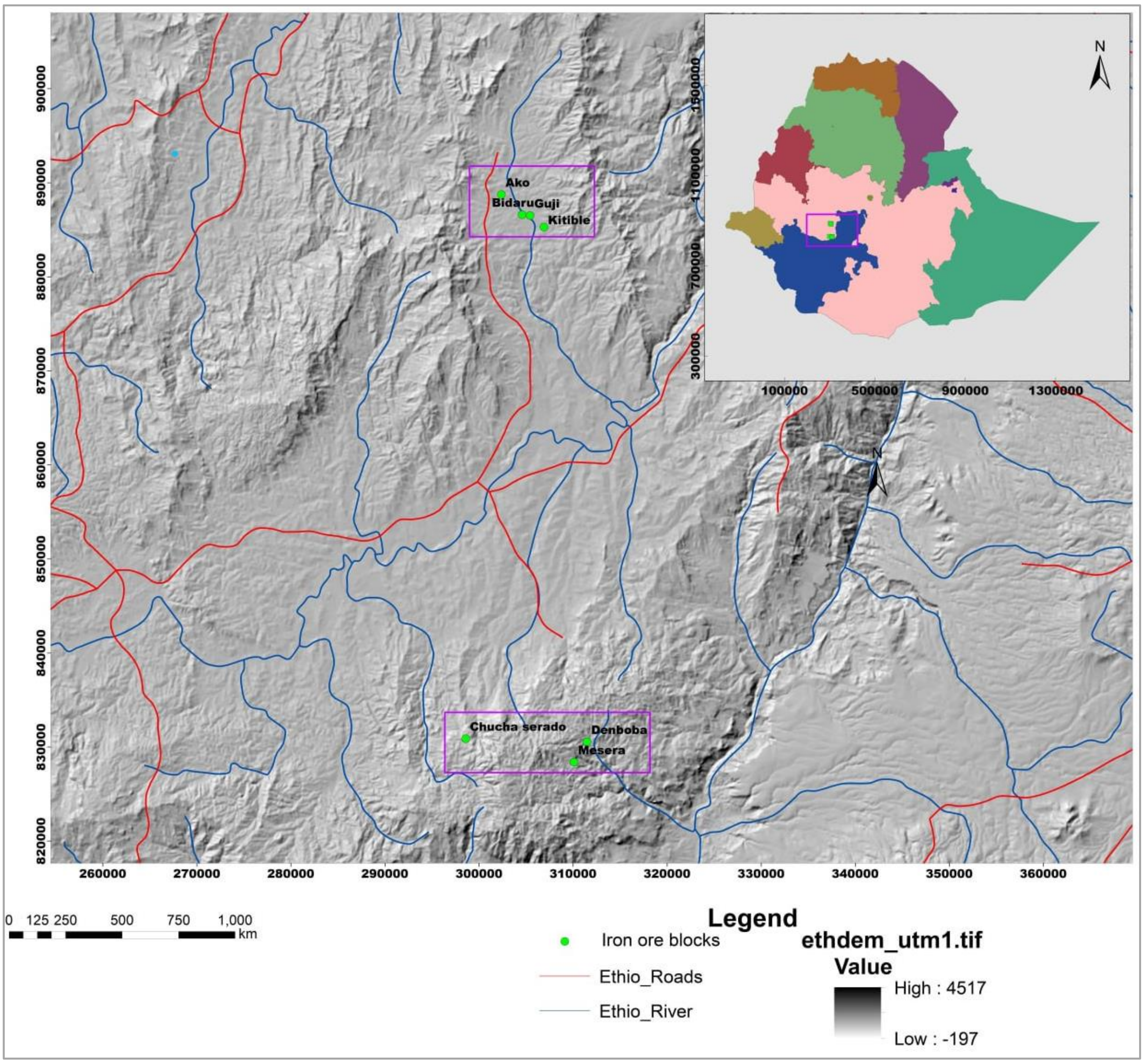

Figure 1. *Location map of the study area.*

In 2021, the Geological Institute of Ethiopia (GIE) carried out an exploration programme in the Omo Beyem and Nedi Gibe woredas, investigating seven lateritic iron targets: Kitimbile, Ako, Bidru, Guji, Chucha Serado, Demboba and Mesera. The present contribution reports the results of that programme and provides the first integrated assessment of the Jimma lateritic iron deposits. The specific objectives are: (1) to describe the geological setting and mode of occurrence of the ore bodies; (2) to determine their mineralogical composition; (3) to characterize their whole-rock geochemistry and weathering intensity using major-oxide data and the Chemical Index of Alteration; and (4) to estimate the contained iron resource.

2. Geological Setting

2.1. Tectonic Framework of the Ethiopian Plateau

The Ethiopian plateau is one of the most extensive tectono-magmatic provinces on Earth, forming part of the larger East African Rift System (EARS). The present-day topography of Ethiopia is dominated by a broadly elevated, ~2-km-high plateau that underwent uplift and incision during and after the Cenozoic flood basalt event in the early Oligocene [9]. The growth of this plateau is intrinsically linked to the impingement of the Afar mantle plume beneath the East African lithosphere at approximately 30 Ma, an event that triggered the rapid eruption of the Ethiopian–Yemen Continental Flood Basalts (CFB) and large-scale basement doming [24, 35].

The Ethiopia–Yemen CFB province covers an area of approximately 600,000 km^2 with an estimated volume exceeding 350,000 km^3 [32, 49]. High-precision $^{40}Ar/^{39}Ar$ geochronology demonstrates that the bulk of the trap volcanism erupted at ca. 30 Ma over a period of 1 Myr or less [13, 24, 36]. These flood basalts are associated with the Afar plume and the initiation of rifting in the southern Red Sea and Gulf of Aden [18, 37]. The plateau-building phase was followed by the formation of the Main Ethiopian Rift (MER), accompanied by bimodal volcanic activity in both the inner parts of the rift and its shoulders [5].

The East African Rift System is of particular interest because sediments trapped in some of the rift depressions have recorded a major piece of late Cenozoic mammalian and hominin evolution, alongside proxies of climate and environmental change. The present-day landscape along the EARS is spectacular and characterised by axial rift valleys surrounded by variously extended volcanic highlands often culminating at altitudes greater than 3,000 m [35]. The morphological development of this unique tectonic and magmatic environment has been increasingly debated and attributed either to (1) the direct and indirect consequences of mantle plume impingement, or to (2) the tectonic and flexural consequences of extensional motion. [35] Argued that most of the elevation of the Ethiopian highlands is inherited from the early Oligocene volcanic and tectonic activities CFB emplacement plus large-scale basement doming triggered by the Afar mantle plume.

The Main Ethiopian Rift itself has a complex structural pattern composed of southern, central and northern segments. Ages of onset of faulting and volcanism indicate a heterogeneous time-space evolution of the segments [3, 7]. Significant rift opening occurred in the central MER during the Pliocene (~5–3 Ma) with the eruption of voluminous ignimbritic covers (the Nazret Sequence) exposed both on the rift shoulders and on the rift floor [7, 10]. Unlike other parts of the MER, Mio-Pliocene silicic volcanism in the MER–Afar transition zone is closely associated with fissural basaltic products [10]. The main rifting phases started diachronously along the MER in the Mio-Pliocene; rift propagation was not a smooth process but rather one with punctuated episodes of extension and relative quiescence [12].

The continental breakup in Afar, where the Red Sea, Gulf of Aden and East African Rift Valley meet at a triple junction, is still an ongoing process. By 4–5 Ma, continental breakup had begun in Afar, with basalts during this period being derived almost entirely from a depleted PREMA-type reservoir [23]. In the Main Ethiopian Rift, where continental breakup is less advanced, young rift basalts retain a geochemical signature consistent with enriched–depleted mantle hybridization [5]. The Afar plume is considered a long-lived feature of the mantle, with volcanic activity persisting over the past 30 million years [19].

2.2. Regional Geology of South-Western Ethiopia

The geology of Ethiopia can be broadly subdivided into four major lithostratigraphic units [6, 42]: (i) the Precambrian crystalline basement belonging to the Arabian–Nubian Shield (ANS) and Mozambique Belt (MB) of the Pan-African orogen (900–500 Ma); (ii) the Palaeozoic to Mesozoic marine and continental sedimentary successions; (iii) the Cenozoic volcanic rocks, including the Oligocene flood basalts and associated felsic volcanics that cover approximately 45% of the country; and (iv) Quaternary to Recent sedimentary and volcanic deposits associated with rifting.

The Precambrian basement of Ethiopia is exposed in four geographically separate zones and has been traditionally classified into three stratigraphic complexes: the Lower Complex (high-grade gneisses representing older cratonic basement, >2.5 Ga), the Middle Complex, and the Upper Complex [27, 44]. The West Ethiopian plateau lies in the transition zone between the Arabian–Nubian Shield and the Mozambique Belt of the Pan-African orogen [48]. The Precambrian basement in the Gimbi–Nejo area consists mainly of intrusive-meta-intrusive and meta-sedimentary rocks, with field evidence indicating four major tectonic stages during the Neoproterozoic era, including rift-valley sedimentation at ca. 980 Ma, lithospheric subduction and arc magmatism at ca. 827 Ma, continental collision at ca. 797 Ma, and late strike-slip deformation at ca. 564 Ma [48]. The Precambrian basement in southern Ethiopia and northern Kenya is characterised by the juxtaposition of the higher-grade Mozambique Belt rocks with the lower-grade Arabian–Nubian Shield rocks, the transition between these two belts being interpreted to represent the root of northward expulsion of the ANS from the Mozambique Belt [40].

Following a prolonged period of erosion and Peneplanation that produced extensive planation surfaces across much of north-east Africa [11], the region experienced the eruption of the Cenozoic volcanic province. In south-western Ethiopia, the Jimma map sheet is dominated by the Jimma Volcanics, a sequence first described in detail by [31] and subsequently refined by Davidson, A [15] and Mengesha et., al [30]. Mohr et al. [33] originally divided the Cenozoic volcanic rocks of Ethiopia into the Trap Series and the Aden Series. The term Trap Series referred to the whole pile of the Tertiary flood basalt sequence with intercalations of felsic lava and pyroclastic rocks (commonly on the upper part), while the Aden Series was confined to mafic lava flows within the younger Afar depression. These names were subsequently modified into groups and formations during later compilations [30].

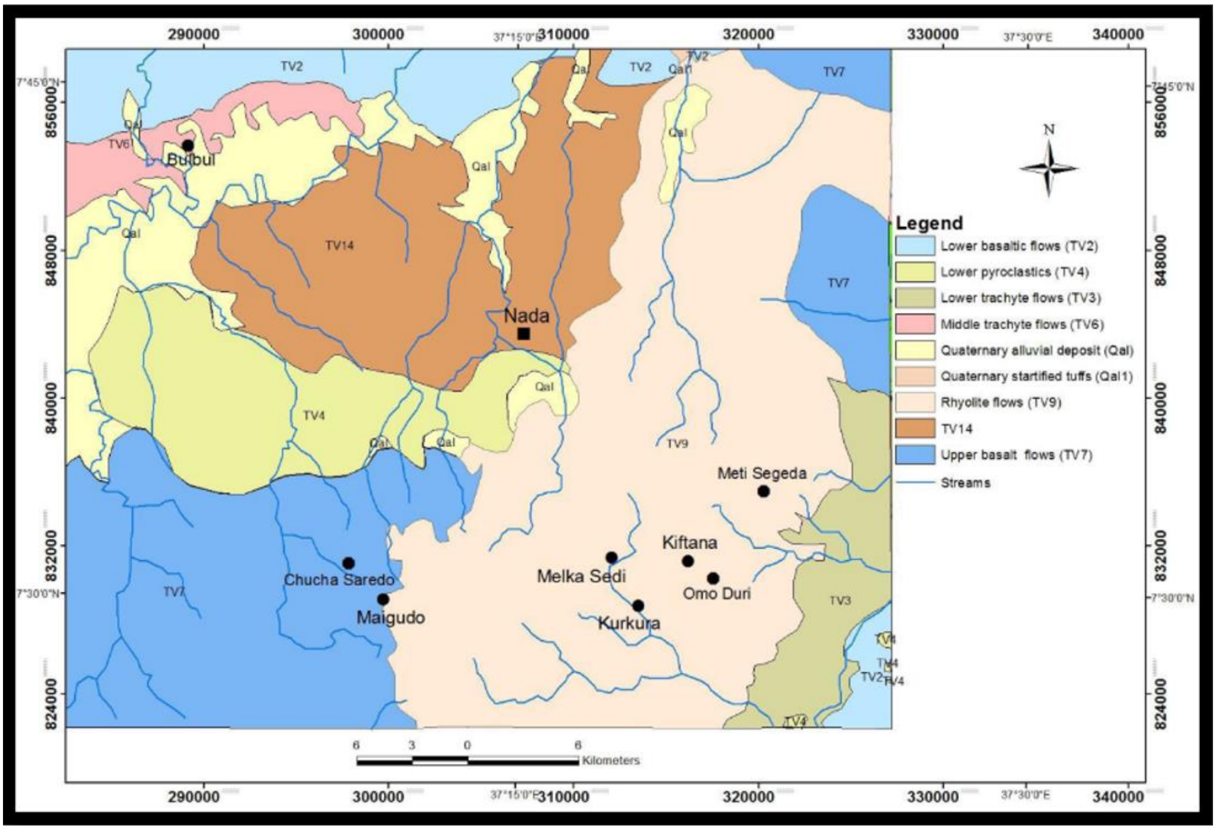

Figure 2. *Regional geology of the area.*

2.3. The Jimma Volcanics: Stratigraphy and Lithology

The Jimma Volcanics were formally defined by Mohr et al [31] as a thick succession of trachybasalts and rhyolites that cover most of south-western Ethiopia. They are considered analogues to the Main Sequence of Davidson, A [15] and form thick successions of basalt and felsic rocks, with basalt dominating the lower part of most sections. Davidson, A [15] Reported K/Ar ages of 42.7 to 30.5 Ma for the Jimma Volcanics, placing their emplacement in the late Eocene to Oligocene. The Jimma Volcanics almost always rest unconformably on the Precambrian basement, with the unconformity being marked by basal residual sandstone in some localities [15, 31].

Two subunits are recognised within the Jimma Volcanics [2, 28]:

1) Lower Jimma Volcanics (Pjb): Dominated by flood basalts with minor silicic flows. The basalts are fine-grained, dark grey, and commonly display columnar jointing. When weathered they exhibit spheroidal weathering and form flat-lying topography. The Omo Basalts, described as mildly alkaline basalts up to 100 m thick, form the lowermost part of this unit and have yielded sparse ages around 30 Ma [16, 31].
2) Upper Jimma Volcanics (Pjr): Dominantly rhyolite and trachyte flows with subordinate basalts, ignimbrites and rare tuffs. These rocks are mainly massive, white, pinkish and grey rhyolites, comendites and pantellerites in thick flows alternating with tuffs [2]. The Upper Jimma Volcanics are equivalent to the Makdela Group of Kazmin, V. [27]. At the Omo village, toward the top of the succession, an age of 27 Ma has been reported [31]. And overall age range of ca. 30 to 27 Ma can be assigned to this unit. Texturally, the rhyolites are fine- to medium-grained and commonly show clear flow banding. The colour variation (white, yellow, red, pink) is due to the oxidation of iron and the presence of K-feldspar.

The Wollega Basalts, resting on the basement and on the tilted Omo Basalts and Jimma Volcanites in the broader south-western region, consist of 200–400 m of predominant columnar alkaline basalt flows interbedded, particularly in the upper portion, with acidic tuffs and loose fluvial-lacustrine deposits; two samples gave ages of 15 and 13 Ma [31].

In the specific study area of the Omo Beyem and Nedi Gibe woredas, the lithologies are basalt, rhyolite, and trachyte [25]. The basalt unit covers a large area and is exposed around Ako town. It is highly to slightly weathered and forms flat topography. The rhyolite unit covers a large area in the southern parts of Omo Nada woreda and is distributed in different localities; it forms rugged topography and is considered the host rock of the vein-form iron mineralization. The trachyte unit is exposed mostly in Omo Nada and Omo Beyem woredas and forms rugged topography with plug-like morphologies having heights of 100–150 m [25].

2.4. Peneplanation and Lateritization in Ethiopia

The formation of lateritic iron deposits on the Ethiopian plateau is intimately linked to the long-term geomorphological evolution of the region. Four major planation surfaces characterize the Ethiopian geology and landscape, having been modeled near or at sea level before the Ordovician, before the Late Triassic, before the Cenomanian, and before the Oligocene [11]. The pre-Oligocene Peneplanation surface (PS4) was of particular significance for lateritization: the Oligocene Trap Volcanics buried a surface of early Tertiary age, which is now widely exposed by erosion.

Before the plume-induced Oligocene uplifts of East/North-east Africa, a relatively long-term Peneplanation happened in Ethiopia after the Cretaceous, during which deep tropical weathering and lateritization could proceed under warm, humid climatic conditions [17]. Only after the onset of rifting processes did uplift become active and transform a vast lowland plain into the present Ethiopian highlands, largely exceeding 2,500 m a.s.l. [11].

The warm, humid climate of the Jimma area (the “Weyna Dega” to “Dega” agro-climatic zones, with mean annual temperatures of 20–25°C and rainfall of up to 2,400 mm yr^{-1}) provides ongoing conditions favorable for deep chemical weathering [25, 38]. Under such conditions, the weathering of ferruginous volcanic protoliths leads to progressive leaching of mobile cations (Ca^{2+}, Na^{+}, K^{+}, Mg^{2+}), desilication, and residual enrichment of the relatively immobile elements Fe, Al and Ti a process known as lateritization [34, 43, 46] The resulting lateritic profiles are characterised by a vertical zonation from unweathered protolith at depth through saprolite and mottled zones to a ferruginous duricrust (ferricrete) at or near the surface [8, 4].

3. Materials and Methods

3.1. Fieldwork and Sampling

Geological mapping was conducted at a scale of 1:5,000. A total of nine trenches (total length 227 m) and eight pits (diameter ~0.7 m, depth 2–3.6 m) were excavated to expose the ore and measure its thickness. Chip and channel samples were collected from outcrops, pit walls, and trench floors at 1–5 m intervals. A total of 192 samples were taken; of these, 147 were submitted for whole-rock major-oxide analysis, and 7 representative ore samples were prepared as polished sections for reflected-light ore microscopy. Bulk density was determined on 11 samples using the water-displacement method.

3.2. Analytical Procedures

Major oxides (SiO_2, Al_2O_3, Fe_2O_3, CaO, MgO, Na_2O, K_2O, MnO, P_2O_5, TiO_2, and LOI) were measured by X-ray fluorescence (XRF) on fused lithium-tetraborate beads at the Central Laboratory of the Geological Institute of Ethiopia. Quality control included duplicate analyses and the use of in-house reference materials. The Chemical Index of Alteration (CIA) was calculated using the molar formula of [34].

$$CIA = Al_2O_3 / (Al_2O_3 + CaO^* + Na_2O + K_2O) \times 100 \quad (1)$$

Where CaO* represents CaO in the silicate fraction only; because all CaO in the analyzed samples is hosted in silicates (carbonate was absent), total CaO was used. The degree of lateritization was assessed using the ternary SiO_2–Al_2O_3–Fe_2O_3 diagram of [39]. The plot was constructed using the mean composition of each deposit.

3.3. Resource Estimation

Resources were estimated using the conventional formula:

$$R = A \times T \times BD \times G \quad (2)$$

Where A is the mapped area of the ore body (m^2), T the average thickness (m), BD the dry bulk density (t m^{-3}), and G the iron grade (Fe%, calculated as 0.7 × Fe_2O_3%). Because the deposits have not been drilled, they are classified as an indicated resource following the guidelines of the Committee for Mineral Reserves International Reporting Standards [14].

4. Results

4.1. Orebody Geometry and Physical Properties

Iron ore is distributed in different volcanic rock units such as basalt, trachyte and rhyolite. These units are the host of iron. The rock fragments of the host are mineralized hematite, which are the result of volcanic and weathering products. The weathered host rocks are exposed at flat and rugged topographic area. The Iron ore in some area is the weathering product of the host rock. It is exposed at flat topographic area, covers large area, has small thickness of black soil overburden, and shows highly to medium weathering and less quality iron ore content. The host rock of this iron ore body at flat area is basalt. However, the iron ore bodies exposed at the rugged topography of the area are the product of volcanic process, which covers small area and has high quality of iron ore. The host rocks of iron ore bodies are trachyte and rhyolite. In this area the iron ore body is also found as coating and vein form (oriented in different direction) on the host rocks.

Mode of Occurrence of the iron mineralization in the Jimma study area occurs in two distinct styles [25]:

1) Lateritic duricrust caps developed on gently undulating terrain underlain by weathered basalt. This style is dominant at Kitimbile, Ako, Bidru and Guji. The ore body is a hard, massive ferruginous crust with oolitic to pisolitic textures, typically 1–5 m thick, and is covered by 0.5–2 m of black soil. Large boulder- to block-sized float ore is common on slopes (Figure 4A, Kitimbile). The protolith for these deposits is the Lower Jimma Volcanics basalt.
2) Vein- and stockwork-type hematite exposed on rugged, elevated ground and hosted by rhyolite and trachyte of the Upper Jimma Volcanics (Chucha Serado, Demboba, and Mesera). The ore bodies are lenticular, 0.5–4 m thick, and commonly show hematite coatings on the wall rock. The mineralization is structurally controlled and displays both concordant and discordant relationships with the host. These higher-grade deposits (Fe_2O_3 up to 70.7%) exhibit evidence of a polyphase origin, with an earlier episode of hydrothermal iron enrichment along fractures that was subsequently upgraded by surface weathering.

Figure 3. *Field exposure of iron mineralization in the study area.*

A summary of the physical parameters of each deposit is presented in Table 1. The largest lateritic bodies are at Kitimbile (0.798 km^2) and Bidru (1.17 km^2). The vein-type deposits at Chucha Serado and Demboba are considerably smaller (0.013–0.014 km^2) but have greater average thicknesses (2.5 m) and higher bulk densities (2.78–3.05 t m^{-3}), reflecting their massive hematite content.

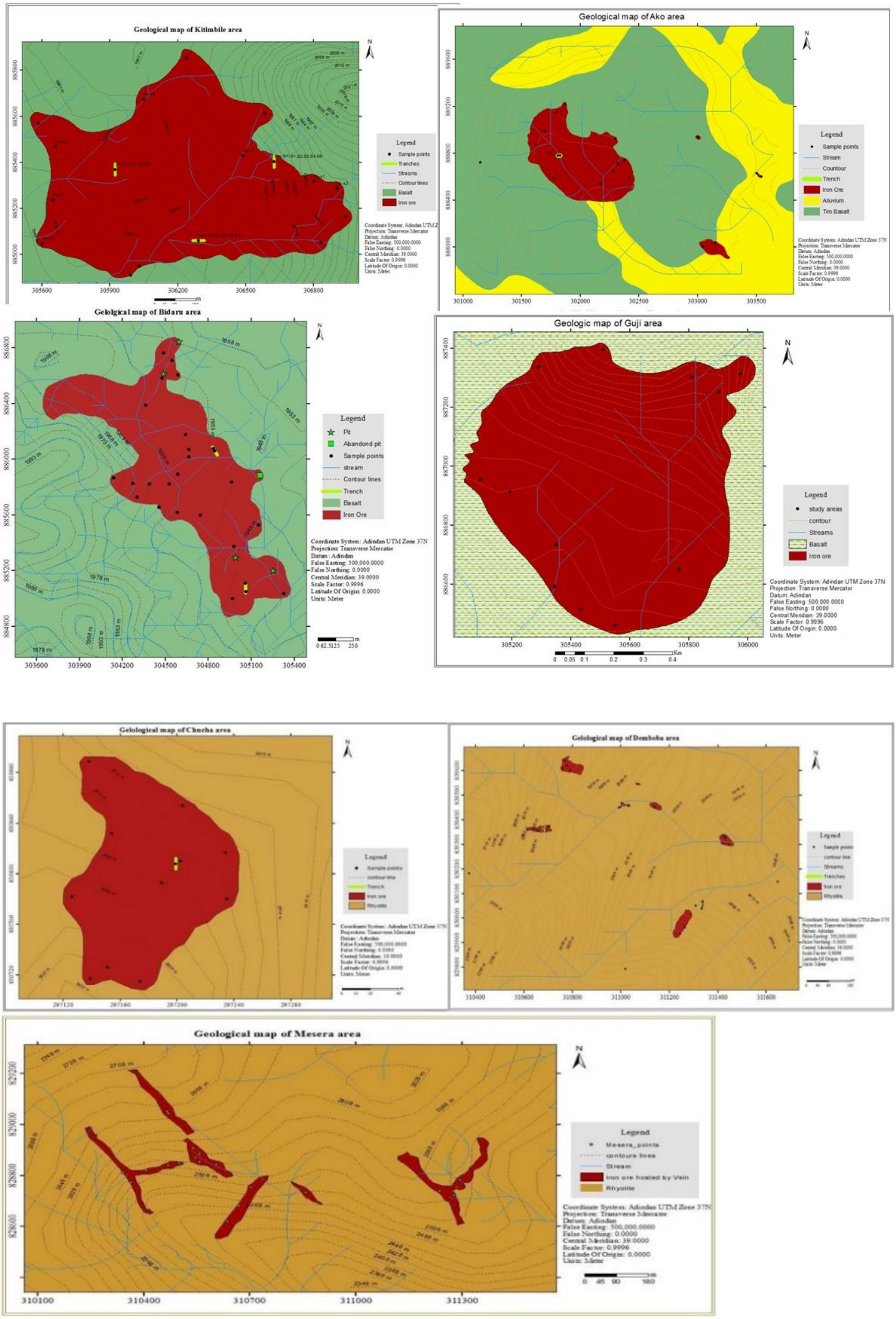

Figure 4. Geological maps of different blocks of iron mineralization in the study area.

Table 1. *Physical parameters of the lateritic iron deposits, Jimma Zone.*

No	Block name	Area (m^2)	Average thickness (m)	Bulk density (g/cm^3)
1	Kitimbile	798,766	1.5	2.04
2	Ako	492,924	1.65	2.07
3	Bidru	1,171,141	1.5	2.31
4	Guji	671,926	1.2	2.57
5	Chucha Serado	14,416	2.5	3.07
6	Demboba	12,914	2.5	2.78
7	Mesera	46,816	1.2	2.57

4.2. Mineralogy

Polished-section examination under reflected light shows that the ore mineralogy is dominated by hematite (30–60%) and goethite (10–35%), with minor magnetite (0.5–5%). Hematite occurs as bladed, specular and ooid interlayers that cement gangue minerals. Goethite forms wavy, platy lenses and colloform aggregates, typical of supergene replacement. The oolitic and pisolitic textures are characteristic of lateritic duricrusts [8]. Gangue minerals identified optically and inferred from bulk chemistry include quartz, kaolinite, and remnants of feldspar.

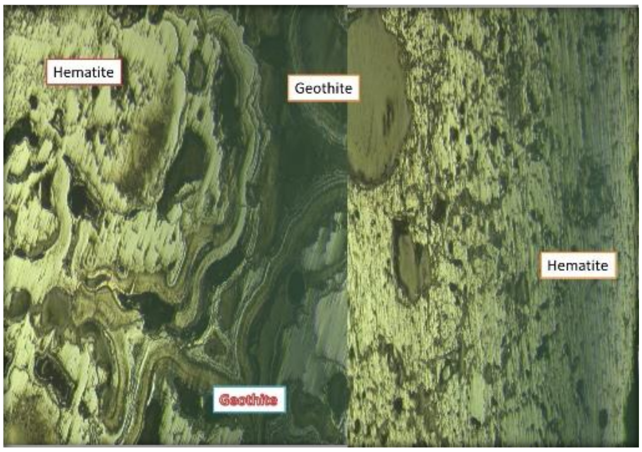

Figure 5. *Reflected microscope photo of iron sample from the study area.*

Hematite appears as layered main ore and dispersed as cementing matrix between the ore and gangues. The hematite ore is characterized by bladed, specular and ooid interlayering texture. The oolith and pisolitic texture of the ore is distorted and perfect ooids with elliptical - rounded hematite. High reflectance, bright color observation is typical features of hematite. In addition to interlayering lenses of goethite grains show wavy and platy appearance to the normal stratification. White to grey white with a bluish tint is typical distinguishing features of hematite ore mineral. The hematite shows moderate reflectance and bright color with fine gangue sediments.

4.3. Whole-Rock Geochemistry

In general iron is found in Fe0, Fe^{2+} and Fe^{3+} forms of highly reduced, reduced and oxidized states respectively. But, ferrous and ferric states of (Fe^{2+} and Fe^{3+}) are the most important once. The reduced and oxidized state of Fe^{2+} and Fe^{3+} determine the types iron ore mineral (Mansurova et al., 2006). The ferrous (Fe^{2+}) is changed to ferric (Fe^{3+}) as it is exposed in to the oxidized environment. In high temperature environment ferrous iron (Fe^{2+}) is substituted by Mn, Mg, Zn, Ni, Ti while ferric (Fe^{3+}) is by Al, V, Ti and Cr. The substitution of ferric (Fe^{3+}) iron in the tetrahedral lattices of alkali feldspar is the main reason for reddish alteration granites during weathering.

Whole rock composition of Jima iron mineralization shows high concentration of Fe_2O_3. It shows very low contents of MnO and P_2O_5 and alkali Earth metal oxides. The weathering of host rock introduced Al_2O_3 and SiO_2 as major oxide. Geochemical analysis shows that iron occurrence is chemically composed of the geochemical fraction of Fe_2O_3, SiO_2, Al_2O_3, and MnO.

Analyzed major content of the ore samples indicate the quality of the iron with average (48.33w%) of Fe_2O_3. The immobile elements (Al, Ti and Fe) especially during weathering and transportation of sedimentary process are forming their relatively moderate-high concentration of oxides. The concentration those oxides are derived from felsic rocks. The total volatile content of the iron ore is determined from the temperature loss in ignition that shows high moderate range of values (i.e. 10.6 average).

The chemical analysis of iron ore samples of study area shows low concentrations of major elements except Fe_2O_3 and

SiO_2. The aluminum content of the iron ore is variable from low (1.44 wt%) to moderate (19.23wt%). Hematite and silica concentration is high. Iron content of the study area ranges from low – high percentage. The iron ore samples generally coupled with moderately low-high beside those major oxides the loss on ignition (LOI) value of iron ore samples are characterized by medium to high concentration.

Major element analysis of the Jimma iron occurrence shows very high quantity of Fe_2O_3, SiO_2 and moderate to high Al_2O_3 content. The high concentration of those major oxides is as a result of laterite process. Because their constituent individual elements are relatively immobile during weathering. The abundant geochemical signatures of those oxides are typical characteristics of laterite iron formation.

The average major-oxide composition for each deposit is given in Table 2; the full dataset is available in the GIE report [25]. Fe_2O_3 contents range from 7.0 wt.% to a maximum of 70.7 wt.% (sample DBS-4, Demboba). The overall mean Fe_2O_3 for the 131 samples is 48.33 wt.%. The highest average grades are found at Chucha Serado (63.00%) and Demboba (52.38%), while the lateritic blankets (Kitimbile, Ako, Bidru, Guji) average 34.6–39.3% Fe_2O_3. SiO_2 is the dominant diluent (overall mean 30.86 wt.%), followed by Al_2O_3 (mean 10.61 wt.%). CaO, MgO, Na_2O and K_2O occur only in trace to minor amounts; their total rarely exceeds 2 wt.%.

Table 2. *Average major-oxide composition (wt.%) of the iron ores from each Block.*

No	Block	n	SiO_2	Al_2O_3	Fe_2O_3	CaO	MgO	Na_2O	K_2O	MnO	TiO_2	LOI
1	Kitimbile	15	32.50	11.50	36.45	0.54	0.23	0.70	1.31	0.70	0.37	10.88
2	Ako	20	30.46	10.71	39.32	3.28	0.39	0.68	1.34	1.78	0.52	10.80
3	Bidru	40	34.26	12.05	34.61	0.81	0.42	1.36	1.20	0.95	0.39	10.35
4	Guji	12	34.15	12.86	36.68	3.74	0.34	0.61	0.32	0.84	0.47	10.69
5	Chucha	4	13.54	10.69	63.00	<0.01	0.12	0.25	0.24	0.12	0.12	10.41
6	Demboba	20	20.96	9.76	52.38	0.52	0.30	0.76	0.92	3.90	0.07	10.88
7	Mesera	20	34.64	6.48	42.74	2.65	0.32	0.64	1.24	1.76	0.11	9.89

n = number of analyzed samples; LOI = loss on ignition.

4.4. Weathering Indices and Lateritization

The CIA values calculated from the average bulk compositions of the most representative lateritic blanket (Bidru) are 88.46% and 89.17%, indicating an advanced degree of chemical weathering. For comparison, CIA values of 100% are typical of heavily leached materials such as tropical laterites and bauxites [34].

On the ternary SiO_2–Al_2O_3–Fe_2O_3 diagram of [39], all seven blocks plot within the "moderate to strong lateritization" field. The high-grade vein deposits (Chucha Serado, Demboba) extend closest to the Fe_2O_3 apex, while the lateritic blankets lie along the trend of increasing desilication. This pattern is consistent with the progressive removal of SiO_2 and the relative accumulation of Fe_2O_3 and Al_2O_3 during tropical weathering [39, 43].

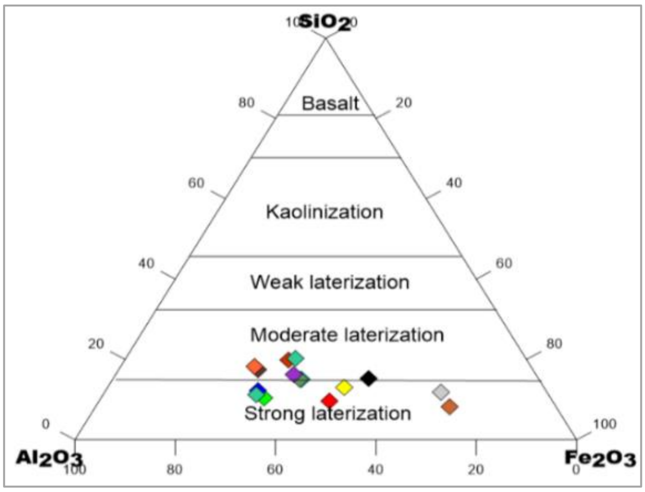

Figure 6. *Ternary Al_2O_3-SiO_2-Fe_2O_3 plot showing different degree of laterizarion for iron bearing rock after [39].*

4.5. Resource Estimation

Applying the measured area, thickness, bulk density, and grade, the indicated resource for each block is summarized in Table 3. The total contained iron metal amounts to approximately 2.7 million tonnes. The largest contributions come from Bidru (0.98 Mt Fe), Kitimbile (0.60 Mt Fe) and Guji (0.53 Mt Fe). Although the high-grade vein deposits are small in volume, their elevated grades (up to 44% Fe) contribute materially to the total metal endowment.

Table 3*. Indicated iron metal resource per block.*

No	block	Volume (m^3)	Grade (Fe fraction)	Contained Fe (tonnes)
1	Kitimbile	1,198,149	0.251	601,470
2	Ako	813,325	0.275	462,985
3	Bidru	1,756,711	0.242	982,036
4	Guji	806,311	0.256	530,488
5	Chucha	36,040	0.440	48,366
6	Demboba	32,285	0.367	32,939
7	Mesera	56,180	0.299	43,170
	Total			2,700,800

5. Discussion

5.1. Genesis of the Jimma Lateritic Iron Deposits

The geological, mineralogical and geochemical data collectively support a predominantly supergene origin for the Jimma deposits. The advanced CIA values (~89%), extreme leaching of alkalis, and residual enrichment of Fe, Al and Ti are hallmarks of intense tropical weathering of ferruginous volcanic protoliths [34, 39]. The oolitic-pisolitic textures and the mineral assemblage hematite + goethite + kaolinite ± quartz are identical to those documented in classic lateritic iron deposits worldwide [8, 47]. These characteristics place the Jimma occurrences in the same genetic category as the Mekaneselam [17] and Mai-Kuhli [21] deposits of the northern Ethiopian plateau, and are broadly comparable to lateritic iron deposits developed on flood basalt provinces elsewhere, such as those of the Deccan Traps in India [47].

The higher-grade, structurally controlled mineralization at Chucha Serado, Demboba and Mesera exhibits evidence of a polyphase origin. The vein and stockwork geometry, the coating of hematite on rhyolite/trachyte walls, and the exceptionally high Fe_2O_3 grades (up to 70.7%) suggest an earlier episode of hydrothermal iron enrichment along fractures, which was subsequently upgraded by surface weathering. This duality hydrothermal protore modified by lateritization is analogous to the process described for the Mentebteb deposit in northern Ethiopia [45].

5.2. Comparison with Other Ethiopian Lateritic Iron Deposits

The Jimma laterites are directly comparable to other documented deposits on the Ethiopian plateau. Mekaneselam averages ~48 wt.% Fe_2O_3 and exhibits similar hematite-goethite-kaolinite mineralogy [17]. Mai-Kuhli reports Fe_2O_3 grades of 45–55 wt.% [21]. The CIA values for Jimma (88.5–89.2%) are slightly lower than the extreme values (>95%) recorded at Mekaneselam, consistent with a somewhat shorter weathering duration or less intense leaching, possibly because the Jimma profiles are developed on both mafic and felsic protoliths. The presence of minor magnetite (up to 5%) in the Jimma ores is a distinguishing feature from the purely hematite-goethite deposits of the north.

The iron ore resources of Ethiopia are widely distributed in different parts of the country, with the most significant deposits including Bikilal (a Kiruna-type magnetite-ilmenite deposit in West Wollega), Melka Arba, Chago, Gordana and Koree [29, 42].

The total inferred iron ore resource of Ethiopia has been estimated at approximately 700 million tonnes, with the largest individual deposit being Bikilal at 58 million tonnes [20]. The Jimma deposits, although individually modest, add a further 2.7 million tonnes of contained iron to the national inventory.

5.3. Economic Potential

With an indicated resource of 2.7 Mt of contained iron, the seven blocks represent a modest but economically attractive target for small-scale mining. The most strategic advantage is their proximity to road infrastructure (40–50 km from Assendabo and connected to the Addis Ababa–Jimma highway) and the availability of water and electricity. The high-grade blocks (Chucha Serado, Demboba) could provide direct-shipping ore or feed for a direct-reduction iron (DRI) plant, while the larger lower-grade blankets (Kitimbile, Bidru) would require simple beneficiation (gravity/magnetic separation) to raise the iron content to >58% Fe_2O_3 [41]. The low concentrations of phosphorus (P_2O_5 average 0.07–0.96%) and sulfur (below detection) are favourable for steelmaking.

5.4. Implications for Further Exploration

The identification of a cluster of lateritic iron deposits in the Jimma Zone extends the known lateritic iron province of the Ethiopian plateau significantly southward. The spatial association with the Upper Jimma Volcanics suggests that similar deposits may exist elsewhere in the region. Remote-sensing analysis using ASTER and Landsat 8 data, successfully applied in northern Ethiopia by [1], could be used to map iron-oxide-rich surfaces and guide further exploration. Follow-up ground geophysical surveys (magnetics, induced polarization/resistivity) and systematic drilling are recommended to upgrade the resource to the measured category and to test the vertical extent of the vein-type mineralization. Furthermore, the potential for rare-earth element enrichment in the lateritic profile, as documented at Mentebteb [45] merits investigation.

6. Conclusion

This study provides the first comprehensive evaluation of the lateritic iron deposits of the Jimma Zone, south-western Ethiopia. The principal findings are:

1) The deposits occur as massive lateritic duricrusts on basalt (Kitimbile, Ako, Bidru, and Guji) and as hematite-rich veins/stockworks in rhyolite and trachyte of the Upper Jimma Volcanics (Chucha Serado, Demboba, and Mesera).
2) Ore mineralogy is dominated by hematite and goethite, with minor magnetite; gangue minerals are quartz and kaolinite.
3) The overall mean Fe_2O_3 content is 48.33 wt.%, with local grades exceeding 70 wt.%. The CIA of 88–89% and the ternary SiO_2–Al_2O_3–Fe_2O_3 diagram indicate a mature laterite profile formed under intense tropical weathering.
4) An indicated resource of 2.7 million tonnes of iron metal is estimated, with the largest tonnages at Bidru, Kitimbile and Guji.
5) The deposits are suitable for small-to-medium-scale exploitation and benefit from favourable infrastructure.

Abbreviations

GIE	Geological Institute of Ethiopia
EARS	East African Rift System
CFB	Continental Flood Basalts
MER	Main Ethiopian Rift
ANS	Arabian–Nubian Shield
MB	Mozambique Belt
XRF	X-ray Fluorescence
CIA	Chemical Index of Alteration
LOI	Loss on Ignition
DRI	Direct Reduction Iron

Acknowledgments

GIE, is Acknowledged for funding the field work and laboratory analysis.

Author Contributions

Yirgalem Hunegnaw: Conceptualization, Data curation, Formal Analysis, Investigation, Methodology, Supervision, Validation, Writing – original draft, Writing – review & editing

Mekdes Taye: Data curation, Formal Analysis, Investigation, Methodology, Software, Visualization, Writing – original draft

Tewodros Tilahun: Data curation, Formal Analysis, Investigation, Methodology, Software, Visualization, Writing – original draft

Habtamu Adugna: Data curation, Formal Analysis, Investigation, Methodology, Software, Visualization, Writing – original draft

Tadesse Tsehaw: Data curation, Formal Analysis, Investigation, Methodology, Software, Visualization, Writing – original draft

Ashenafi Yazew: Data curation, Formal Analysis, Investigation, Methodology, Software, Visualization, Writing – original draft

Dessalew Mengistie: Data curation, Formal Analysis, Investigation, Methodology, Software, Visualization, Writing – original draft

Funding

This work was fully funded by the Geological Institute of Ethiopia, Ministry of Mines.

Data Availability Statement

The original contributions presented in the study are included in the article and in the GIE internal report further inquiries can be directed to the corresponding author.

Conflicts of Interest

The authors declare no conflicts of interest.

References

[1] Abay, H. H., Legesse, D., Suryabhagavan, K. V., and Atnafu, B. (2022). Mapping of ferric (Fe^{3+}) and ferrous (Fe^{2+}) iron oxides distribution using ASTER and Landsat 8 OLI data, in Negash lateritic iron deposit, Northern Ethiopia. Geocarto Int. 37, 13058–13079. https://doi.org/10.1080/10106049.2022.2071474

[2] Abbate, E., and Sagri, M. (1980). The volcanites of the Ethiopian and Somali plateaus: major and trace element geochemistry. Atti Convegni Lincei 47, 213–231.

[3] Abebe, T., Manetti, P., Bonini, M., Corti, G., Innocenti, F., and Mazzarini, F. (2007). Geological map (scale 1:200,000) of the northern Main Ethiopian Rift. J. Maps 3, 168– 187.

[4] Beauvais, A., and Colin, F. (1993). Formation and transformation processes of iron duricrust systems in tropical humid environment. Chem. Geol. 107, 471–474. https://doi.org/10.1016/0009-2541(93)90242-B

[5] Beccaluva, L., Bianchini, G., Coltorti, M., Siena, F., and Zerbi, M. (2005). The Ethiopian subcontinental mantle domains: geochemical evidence from Cenozoic mafic lavas. Mineral. Petrol. 84, 35–59. https://doi.org/10.1007/s00710-005-0088-4

[6] Billi, P. (2015). Landscapes and Landforms of Ethiopia. Dordrecht: Springer. https://doi.org/10.1007/978-94-017-8026-1

[7] Bonini, M., Corti, G., Innocenti, F., Manetti, P., Mazzarini, F., Abebe, T., and Pecskay, Z. (2005). Evolution of the Main Ethiopian Rift in the frame of Afar and Kenya rifts propagation. Tectonics 24, TC 1007. https://doi.org/10.1029/2004TC001680

[8] Boudeulle, M., and Muller, J. P. (1988). Structural characteristics of hematite and goethite and their relationship with kaolinite in laterite from Cameroon. Bull. Minéral. 111, 149–166.

[9] Bowden, S., Gani, N. D., Furman, T., Gani, M. R., VanSoest, M., Abebe, T., et al. (2022). Feedback between topography and lithosphere–asthenosphere dynamics beneath the Yerer-Tulu Wellel volcano-tectonic lineament. Geol. J. 57, 3569–3586. https://doi.org/10.1002/gj.4488

[10] Chernet, T., Hart, W. K., Aronson, J. L., and Walter, R. C. (1998). New age constraints on the timing of volcanism and tectonism in the northern Main Ethiopian Rift–southern Afar transition zone (Ethiopia). J. Volcanol. Geotherm. Res. 80, 267–280. https://doi.org/10.1016/S0377- 0273(97)00049-8

[11] Coltorti, M., Pieruccini, P., Dramis, F., and Ollier, C. D. (2015). "Planation surfaces and the long-term geomorphological evolution of Ethiopia," in Landscapes and Landforms of Ethiopia, ed. P. Billi (Dordrecht: Springer), 78–96. https://doi.org/10.1007/978-94-017-8026-1_4

[12] Corti, G. (2009). Continental rift evolution: from rift initiation to incipient break-up in the Main Ethiopian Rift, East Africa. Earth-Sci. Rev. 96, 1–53. https://doi.org/10.1016/j.earscirev.2009.06.005

[13] Coulié, E., Quidelleur, X., Gillot, P. Y., Courtillot, V., Lefèvre, J. C., and Chiesa, S. (2003). Comparative K–Ar and Ar/Ar dating of Ethiopian and Yemenite Oligocene volcanism: implications for timing and duration of the Ethiopian traps. Earth Planet. Sci. Lett. 206, 477–492. https://doi.org/10.1016/S0012-821X(02)01084-1

[14] CRIRSCO (2019). International Reporting Template for the Public Reporting of Exploration Results, Mineral Resources and Mineral Reserves. Available at: www.crirsco.com

[15] Davidson, A. (1983). The Omo River Project: Reconnaissance Geology and Geochemistry of Parts of Ilubabor, Kefa, Gemu Gofa and Sidamo, Ethiopia. Ethiopian Institute of Geological Surveys, Addis Ababa.

[16] Davidson, A., and Rex, D. C. (1980). Age of volcanism and rifting in southwestern Ethiopia. Nature 283, 657–658. https://doi.org/10.1038/283657a0

[17] Digafe, B., Getaneh, W., and Atnafu, B. (2024). Lateritization and enrichment of ferruginous protore during the peneplanation between uplifts – the case of Mekaneselam iron deposit, NW Ethiopian plateau. Geol. Ecol. Landscapes 9 (1), 1365–1381. https://doi.org/10.1080/24749508.2024.2429207

[18] Ebinger, C. J., and Sleep, N. H. (1998). Cenozoic magmatism throughout East Africa resulting from impact of a single plume. Nature 395, 788–791. https://doi.org/10.1038/27417

[19] Furman, T., Bryce, J., Karson, J., and Iotti, A. (2006). Heads and tails: 30 million years of the Afar plume. Geol. Soc. London Spec. Publ. 259, 95–120. https://doi.org/10.1144/GSL.SP.2006.259.01.08

[20] Geological Survey of Ethiopia (2010). Geoscience Data Center: Iron Ore Occurrences of Ethiopia. Addis Ababa: GSE.

[21] Gidey, T., Hagos, M., Konka, B., Gebremicale, A., and Bheemalingeswara, K. (2020). Genesis and characteristics of lateritic iron deposit in Mai-Kuhli area, western Tigray, northern Ethiopia. J. Afr. Earth Sci. 171, 103967. https://doi.org/10.1016/j.jafrearsci.2020.103967

[22] Hamrla, H. (1966). The Iron Ore Deposits of Ethiopia. Addis Ababa: Ministry of Mines.

[23] Hart, W. K., WoldeGabriel, G., Walter, R. C., and Mertzman, S. A. (1989). Basaltic volcanism in Ethiopia: constraints on continental rifting and mantle interactions. J. Geophys. Res. 94, 7731–7748. https://doi.org/10.1029/JB094iB06p07731

[24] Hofmann, C., Courtillot, V., Féraud, G., Rochette, P., Yirgu, G., Ketefo, E., and Pik, R. (1997). Timing of the Ethiopian flood basalt event and implications for plume birth and global change. Nature 389, 838–841. https://doi.org/10.1038/39853

[25] Hunegnaw, Y., Taye, M., Tilahun, T., Adugna, H., Tsehaw, T., Yazew, A., and Mengistie, D. (2022). Iron Ore Exploration in Omo Beyem and Nedi Gibe Woreda, Jimma Zone, Oromia National Regional State. Unpublished internal report, Geological Institute of Ethiopia, Addis Ababa.

[26] Kabeto, K., Seid, M., and Mogessie, A. (2013). Petrography and geochemistry of ferricrete near Shire, northern Ethiopia. Momona Ethiop. J. Sci. 5 (2), 5–29.

[27] Kazmin, V. (1972). Geological Map of Ethiopia, Scale 1:2,000,000. Addis Ababa: Geological Survey of Ethiopia.

[28] Kim, Y., Lee, C., and Park, S. (2022). Global iron ore market and supply security. Resour. Policy 78, 102872. https://doi.org/10.1016/j.resourpol.2022.102872

[29] Mammo, J. (2013). Geology, Mineral Paragenesis and Sequence Study of Bikilal Iron Mineralization in West Wollega, Western Ethiopia: Implication to Genesis. MSc thesis, Addis Ababa University.

[30] Mengesha, T., Chernet, T., and Haro, W. (1996). Explanation of the Geological Map of Ethiopia. Bull. Geol. Surv. Ethiop. 3, 1–79.

[31] Merla, G., Abbate, E., Azzaroli, A., Bruni, P., Canuti, P., Fazzuoli, M., et al. (1979). A Geological Map of Ethiopia and Somalia (1973) and Comment. Firenze: CNR.

[32] Mohr, P. A. (1963). The geology of Ethiopia. Bull. Geophys. Obs. Addis Ababa 5, 97–157.

[33] Mohr, P. A. (1983). Ethiopian flood basalt province. Nature 303, 577–584. https://doi.org/10.1038/303577a0

[34] Nesbitt, H. W., and Young, G. M. (1982). Early Proterozoic climates and plate motions inferred from major element chemistry of lutites. Nature 299, 715–717. https://doi.org/10.1038/299715a0

[35] Pik, R., Bellahsen, N., Leroy, S., Denèle, Y., and Ayalew, D. (2010). Uplift, rifting and related geomorphological evolution of the Ethiopian volcanic province: what do we really know? AGU Fall Meet. Abstr. T 23F-04.

[36] Rochette, P., Tamrat, E., Féraud, G., Pik, R., Courtillot, V., Ketefo, E., et al. (1998). Magnetostratigraphy and timing of the Oligocene Ethiopian traps. Earth Planet. Sci. Lett. 164, 497–510. https://doi.org/10.1016/S0012-821X(98)00226-X

[37] Rogers, N., Macdonald, R., Fitton, J. G., George, R., Smith, M., and Barreiro, B. (2000). Two mantle plumes beneath the East African rift system: Sr, Nd and Pb isotope evidence from Kenya Rift basalts. Earth Planet. Sci. Lett. 176, 387–400. https://doi.org/10.1016/S0012-821X(00)00012-1

[38] RTI (Radar Technologies International) (2014). A National Shallow Groundwater Mapping Exercise: Central Ethiopia, Including Woredas in Oromiya and Southern Regions. Draft Final Report.

[39] Schellmann, W. (1986). A new definition of laterite. Geol. Surv. India Mem. 120, 1–7.

[40] Shackleton, R. M. (1992). Northward expulsion of the Pan-African of northeast Africa guided by a reentrant zone of the Tanzania craton. Geology 20, 1023–1026. https://doi.org/10.1130/0091-7613(1992)020<1023:NE-OTPA>2.3.CO;2

[41] Srivastava, J. P., and Pathak, P. N. (2000). “Beneficiation of low-grade iron ores,” in Mineral Processing: Recent Advances and Future Trends, eds. S. K. Jain and R. Singh (New Delhi: Allied Publishers), 247–255.

[42] Tadesse, S., Milesi, J. P., and Deschamps, Y. (2003). Geology and mineral potential of Ethiopia: a note on geology and mineral map of Ethiopia. J. Afr. Earth Sci. 36, 273–313. https://doi.org/10.1016/S0899-5362(03)00048-4

[43] Tardy, Y. (1997). Petrology of Laterites and Tropical Soils. Rotterdam: Balkema.

[44] Teklay, M., Kröner, A., and Mezger, K. (2007). Evidence of pre-Pan-African crustal components in migmatitic biotite gneiss and granitic orthogneisses of the western Ethiopian Precambrian basements. J. Mineral. Petrol. Sci. 102, 198–207. https://doi.org/10.2465/jmps.061123

[45] Tesfaye, B., Kebede, A., Assefa, W., and Dibaba, M. (2025). Major, trace, and Rare Earth Element (REE) characteristics of the Mentebteb lateritic iron deposit, northern Ethiopia. Geochem. Explor. 269, 105672. https://doi.org/10.1016/j.gexplo.2025.105672

[46] Widdowson, M. (2009). “Laterite and ferricrete,” in Encyclopedia of Geology, eds. R. C. Selley, L. R. M. Cocks, and I. R. Plimer (Amsterdam: Elsevier), 335–345. https://doi.org/10.1016/B978-0-12-409548-9.12578-X

[47] Widdowson, M., and Cox, K. G. (1996). Uplift and erosional history of the Deccan Traps, India: evidence from laterites and drainage patterns of the Western Ghats and Konkan coast. Earth Planet. Sci. Lett. 137, 57–69. https://doi.org/10.1016/0012-821X(95)00211-T

[48] Woldemichael, S., Tadesse, A., and Bedada, T. (2024). Geochronology, geochemistry, and tectonic setting of the Neoproterozoic magmatic rocks in Pan-African basement, West Ethiopia. Ore Geol. Rev. 164, 105858. https://doi.org/10.1016/j.oregeorev.2023.105858

[49] Zanettin, B. (1993). On the evolution of the Ethiopian volcanic province. Mem. Sci. Geol. 45, 79–98.